J. theor. Biol. (1990) **145,** 183–198

Electrostatic Potential Maps at the Quantum Chemistry Level of the Active Sites of the Serine Peptidases, α-Chymotrypsin and Subtilisin

JOSETTE LAMOTTE-BRASSEUR, GEORGES DIVE, DOMINIQUE DEHARENG AND JEAN-MARIE GHUYSEN†

Service de Microbiologie, Université de Liège, Institut de Chimie, B6, B-4000 Sart Tilman (Liège 1), Belgium

(*Received on* 25 *August* 1989, *Accepted on* 7 *December* 1989)

The electronic properties of the active-sites of the structurally unrelated serine peptidases, α-chymotrypsin and subtilisin, have been expressed in the form of three-dimensional electrostatic potential maps derived from integrals calculated at the quantum chemistry level. As a consequence of the asymmetrical distribution of the secondary structures that occur within a 7 Å sphere around the serine of the catalytic triad, the active sites are highly polarized entities and exhibit large dipole moments. One part of the active sites generates a nucleophilic suction-pump. Its isocontour at -10 kcal mol^{-1} defines an impressive, negatively-charged volume which bears a narrow channel in the immediate vicinity of the active-site serine 195 in α-chymotrypsin or 221 in subtilisin. In native α-chymotrypsin, there is a perfect complementation between this nucleophilic suction-pump and the positively-charged electrophilic hole that is generated by the backbone NH of Ser 195 and Gly 193. In subtilisin, generation of the complementing electrophilic hole requires binding of a carbonyl donor ligand and may be achieved by rotation of the side-chain amide of Asn 155 towards the backbone NH of Ser 221. Small variations in the atomic co-ordinates of α-chymotrypsin used for the calculations, the presence of water molecules in its active site and the occurrence of point mutations in the amino acid sequence of subtilisin have little effects on the shape and characteristics of the electrostatic potential.

Introduction

Serine-peptidases-catalysed rupture of a peptide bond in a susceptible carbonyl donor R-CONH-R′ is made by transfer of the R-CO-electrophilic group to an essential serine and then to an exogenous acceptor. Central to this mechanism is the formation of a serine-ester linked acyl enzyme. This reaction is carried out by several enzyme reagents that fulfil distinct functions. An electrophile or oxyanion binding site polarizes the carbonyl oxygen atom of the scissile bond and a proton abstractor-donor enhances the reactivity of the Oγ of the essential serine thus permitting nucleophilic attack of the carbonyl carbon atom and, concomitantly, achieves protonation of the nitrogen atom. The serine peptidases of the trypsin and subtilisin families though lacking relatedness in the primary and three-dimensional structure, have similarities in the active-site configuration and have evolved a similar catalytic device characterized by the Ser His Asp triad.

† Author to whom all correspondence should be addressed.

0022-5193/90/014183+16 $03.00/0

Based on the atomic co-ordinates of the proteins, α-chymotrypsin of the trypsin family and subtilisin have been the topic of many studies aimed at defining their mode of action. In particular, a satisfying picture of the interaction of α-chymotrypsin with N-acetyl-L-tryptophanamide has been produced by the molecular mechanics studies of Wipff *et al.* (1983), in which the total energy of the non-covalent Michaelis complex has been minimized with respect to all degrees of freedom. Almost every property of subtilisin, from *Bacillus amyloliquefaciens*, has been altered by protein engineering including its catalysis, substrate profile, pH/rate profile and stability to oxidation, thermal and alkalin inactivation (Wells & Estell, 1988). Differential free energy of binding and free energy of activation for catalysis by both the native enzyme and a mutant where the Ala replacement of Asn 155 perturbs the oxyanion binding site, have been calculated by a free energy perturbation method (Rao *et al.*, 1987).

At each point of the three-dimensional map of a molecule, the electrostatic potential expresses the value of the electrostatic energy of the interaction with a unitary positive charge. The electrostatic potential isocontours can be regarded as the best intrinsic fingerprint of the molecule under consideration since it takes into account its volume, conformation and electronic distribution. In the work which is presented here, the active sites of α-chymotrypsin and subtilisin have been identified by the 3-D electrostatic potentials derived from integrals calculated at the quantum chemistry level. The active sites are defined by those amino acids which lie within a 7 Å sphere around the essential serine, each of them occupying that spatial disposition shown by X-ray crystallographic studies. In addition, the occurrence of water molecules within the active site of α-chymotrypsin has been taken into account.

Materials and methods

DEFINITION OF THE ACTIVE SITES AND SELECTED MODELS

α-Chymotrypsin

Two sets of atomic co-ordinates were used. Those kindly provided by Dr G. Wipff were obtained by molecular mechanics energy refinement (Wipff *et al.*, 1983) of the X-ray crystal structure at 2 Å resolution (Birktoft & Blow, 1972). In these calculations, Trp 215 whose side-chain protrudes outside the active site, was replaced by Gly. This point replacement was also kept in the present study. The second set of atomic co-ordinates derived from the X-ray crystal structure refined at 1·68 Å resolution by Tsukada & Blow (1985).

The α-chymotrypsin active site is defined by the 22 amino acids listed in Table 1. Their spatial disposition is shown in Fig. 1(a). Gly 226, Val 227 and Tyr 228 are at the boundary of the cleft. His 57, Asp 102 and Ser 195 form the catalytic triad. The backbone NH of Ser 195 and that of Gly 193 create the required electrophile. The β-strand Val 213 Ser 214 Gly 215 Gly 216 serves as binding site for peptide ligands. Two S–S bridges occur between Cys 42 and Cys 58 and between Cys 191 and Cys 220.

TABLE 1

Amino acids occurring within a 7 Å sphere around the active serine of α-chymotrypsin (Ser 195) and subtilisin (Ser 221)

	Chymotrypsin			Subtilisin	
	CHT1	CHT2	CHT3		
Cys 42			+	Asp 32	+
Gly 43			+		
				His 64	+
Ala 55			+		
Ala 56	+	+	+	His 67	+
His 57	+	+	+	Val 68	+
Cys 58			+		
				Ser 125	+
Asp 102	+	+	+	Leu 126	+
				Gly 127	+
Ser 190			+		
Cys 191		+	+	Ala 152	+
Met 192		+	+	Ala 153	+
Gly 193	+	+	+	Gly 154	+
Asp 194			+	Asn 155	+
Ser 195	+	+	+		
Gly 196		+	+	Gly 178	+
				Ala 179	+
Val 213		+	+		
Ser 214	+	+	+	Tyr 217	+
Gly 215†		+	+	Asn 218	+
Gly 216		+	+	Gly 219	+
				Thr 220	+
Cys 220		+	+	Ser 221	+
				Met 222	+
Gly 226		+		Ala 223	+
Val 227		+		Ser 224	+
Tyr 228		+			

† Trp occurs at position 215 in α-chymotrypsin (see text).

The electrostatic potential of the α-chymotrypsin active site was computed for three models of increasing completeness (Table 1) referred to as CHT1 (six amino acids, 91 atoms), CHT2 (16 amino acids, 207 atoms) and CHT3 (19 amino acids, 216 atoms) using the co-ordinates of Wipff *et al.* (1983), and CHT3-TB using the co-ordinates of Tsukada & Blow (1985). In addition, the nine crystallization water molecules putatively identified in the X-ray structure were introduced in model CHT3-TB (yielding model CHT3-TB-9 H_2O) and 25 water molecules selected from a Monte Carlo water bath (Amber program) were introduced in model CHT3 (yielding model CHT3-25 H_2O), thus filling up all the available space.

Subtilisin

The atomic co-ordinates derived from the X-ray crystal structure of subtilisin Novo (Drenth *et al.*, 1972). The active-site is defined by the 21 amino acids listed in Table 1. Their spatial disposition is shown in Fig. 1(b). Asp 32, His 64 and Ser

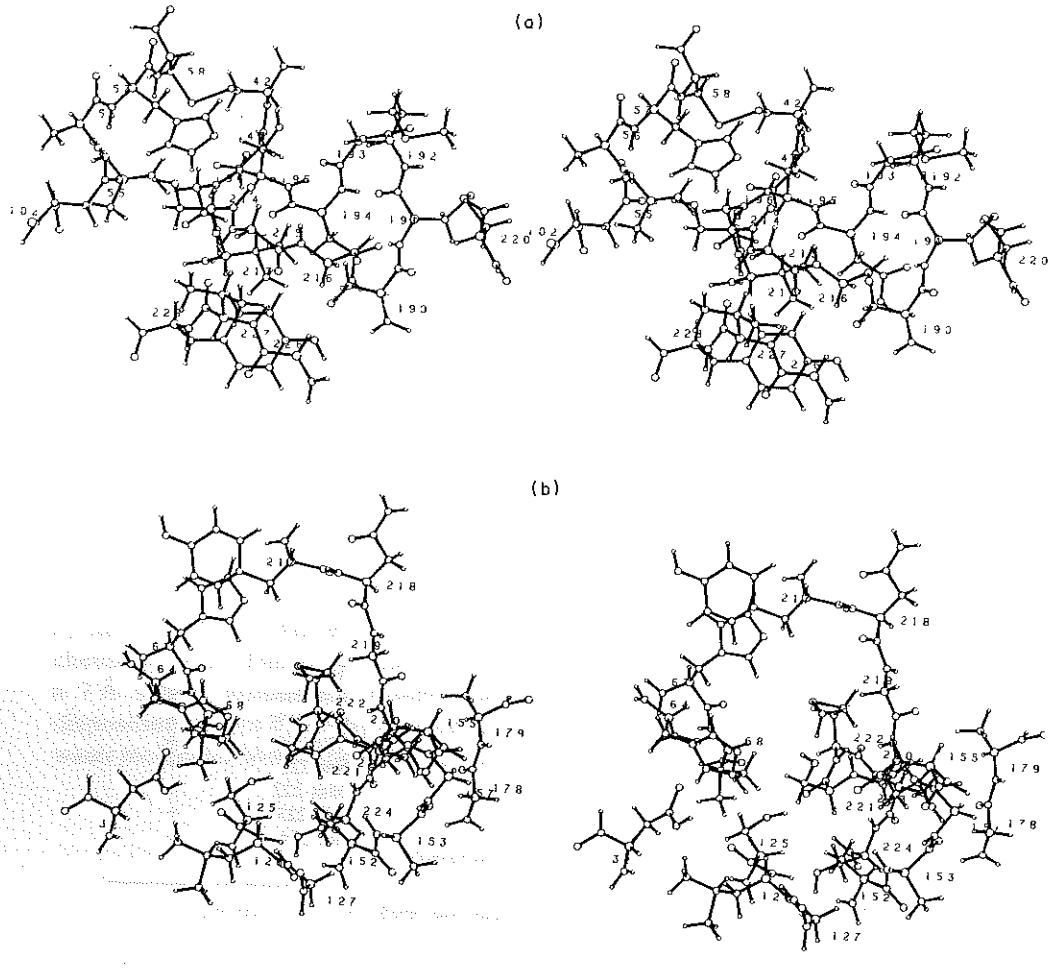

FIG. 1. 3-D Structure of the active sites of α-chymotrypsin (a) and subtilisin (b). The active sites are defined by the 22 residues (α-chymotrypsin) and 21 residues (subtilisin) listed in Table 1.

221 form the catalytic triad. The backbone NH of Ser 221 and the side-chain of Asn 155 create the required electrophile (upon binding with a suitable ligand). The β-strand Ser 125 Leu 126 Gly 127 is involved in substrate binding. The maps were computed for the native enzyme (21 amino acids, 277 atoms) and for three mutants with single Ala replacement of His 64 and Ser 221 of the catalytic triad, and of Ser 125 (Table 1).

With both α-chymotrypsin and subtilisin, the electrostatic potential maps were those of total valence satisfied molecules. Consequently, the NH and CO groups artificially created at the ends of the selected peptide stretches (Table 1) were converted into NH_2 and either COH or $COCH_3$ groups.

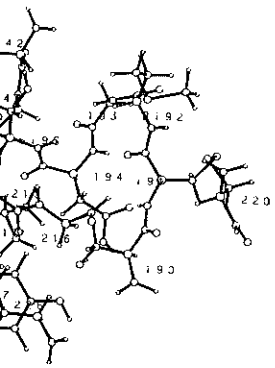

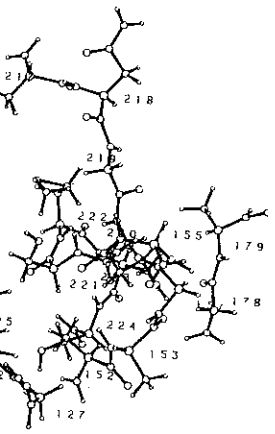

n (b). The active sites are
l in Table 1.

nd the side-chain of
suitable ligand). The
ling. The maps were
nd for three mutants
ytic triad, and of Ser

potential maps were
NH and CO groups
hes (Table 1) were

THEORETICAL BACKGROUND

General equations

The electrostatic field **E** and the electrostatic potential V are given by;

$$\nabla \cdot \mathbf{E} = -\nabla \cdot (\nabla V) = 4\pi\rho, \tag{1}$$

where ρ is the charge distribution.

In the quantum chemistry framework, V at point r is expressed by;

$$V(r) = \sum_{\mu}\sum_{\nu} D_{\mu\nu} \int \mathrm{d}r' \chi_{\mu}(r') \frac{1}{|r-r'|} \chi_{\nu}(r') + \sum_{\alpha} \frac{Z_{\alpha}}{|r-R_{\alpha}|}, \tag{2}$$

where $D_{\mu\nu}$ are the density matrix elements and $\chi_{\mu}(r')$ the atomic orbitals.

In the point charge framework, V at point r is expressed by;

$$V(r) = \sum_{i} \frac{q_i}{|r-R_i|}, \tag{3}$$

where q_i are point charges at position R_i, which point charges are often chosen as the net charges localized on the atoms.

Microscopic vs. macroscopic treatment of eqn (1)

Microscopic treatment of eqn (1) implies that each particle of the system explicitly contributes to ρ. $V(r)$ can be defined using eqns (2) or (3). In contrast, macroscopic treatment of eqn (1) implies that ρ is immerged in a continuum medium the properties of which are considered as an average of all the constitutive elements. One of the electrostatic properties is characterized by a dielectric constant ε the value of which expresses the ability of the medium to stabilize the isolated charges. The charge distribution ρ polarizes the environment and forces the dipoles of the medium to orient according to the electrostatic field generated by ρ. Reciprocally, the counteracting action of the medium exerts a screening effect on ρ. Hence eqn (1) becomes;

$$\nabla \cdot \mathbf{E} = -\nabla \cdot (\nabla V) = 4\pi(\rho - \nabla \cdot \mathbf{P}) = 4\pi \frac{\rho}{\varepsilon} = 4\pi\rho^{\mathrm{eff}}, \tag{4}$$

where ρ^{eff} is the effective charge distribution and **P** is the polarizability of the medium.

Study of the possible influence that a solvent exerts on the electrostatic potential of a given macromolecule can be made using either the microscopic or the macroscopic treatment. However, the macroscopic treatment is justified only if the two following conditions are fulfilled: a large number of solvent molecules must be present and the distances between the interacting partners must be larger than the interatomic distances. Such conditions do not apply to enzyme active sites. Indeed, they contain few solvent, i.e. water molecules (25 at the most in the case of chymotrypsin; see above) and the distances under consideration are of the same order of magnitude.

Use of a dielectric constant as a screening function

Many authors introduce a dielectric constant in their point charge model (eqn (3)] for the calculation of the electrostatic interactions in proteins. They do so by

reference to the work of Warshell & Levitt (1976) on lysozyme. In fact, the screening function, conceptually similar to a dielectric constant, which was used in this work did not serve to calculate the Coulombic electrostatic term but served only to calculate the polarization energy between the enzyme active site which was treated at the quantum level and the rest of the protein which was treated as a continuum.

When the charges of a polypeptide chain are those obtained from each isolated amino acid, one could assume that the combined effect of these charges in the folded polypeptide creates a polarization that modulates their initial incidence so that, at first sight, the use of such a screening dielectric function would be justified for expressing the electrostatic monopole–monopole term of the interaction energy and/or the electrostatic potential. It remains that the use of this dielectric function is not relevant if the charges of the amino acids under consideration are obtained from a self-consistent quantum chemistry calculation carried on the whole polypeptide since this procedure takes into account all possible effects such as polarization, exchange repulsion and charge transfer. The significance of these self-consistent charges was addressed by calculating from eqn (3) the electrostatic potential of the six amino acid CHT1 model of α-chymotrypsin (in which Asp 102 was aspartic acid) using the net charges derived from a CNDO calculation carried on the whole hexapeptide and followed by a Mulliken population analysis. The electrostatic potential was then compared with that obtained from net charges of the six isolated amino acids. This latter procedure generated negatively charged domains which, at the level of -10 kcal mol^{-1}, were homogeneously distributed around the hexapeptide without any preferential localization. In contrast, as a direct consequence of the self-consistency of the charges, the first procedure revealed co-operativity between certain carbonyl groups. It generated well-defined negative wells around the carbonyl group of Gly 193, that of Ser 195, the Oγ of Ser 214 and around the two nitrogen atoms of the imidazole ring of His 57 (not shown). The unexpected occurrence of negative wells around His 57 showed that, even with self-consistent charges, the point charge framework [eqn (3)] does not take into account the interaction of His 57 with the neighbouring Ser 195 and Asp 102. Hence, even this model is misleading and a correct description of the electrostatic property necessitates the integral expression of the potential itself [eqn (2)].

As a conclusion of the above analysis, the electrostatic potentials of the serine peptidases were calculated in a consistent quantum chemistry framework by solving the electrostatic integral expression [eqn (2)], without any screening function. When water molecules were introduced in the active site, ρ was defined by the contribution of both the amino acids that form the active site and the water molecules.

As a whole entity, an enzyme active site is electrically neutral because of the counterions neutralizing effect. Since their positions are not known, the polarization which is induced by these counterions and the charged residues is assumed to be fulfilled by the dielectric constant. In order to check how accurately ε can take into account the effect of the charged residues on the polarization response of the molecule, the electrostatic potential of the CHT1 model of α-chymotrypsin was calculated in the point charge framework [eqn (3)] with the isolated net charges, assuming that (i) Asp 102 is aspartic acid and $\varepsilon = 1$ [Fig. 2(a)]; (ii) Asp 102 is

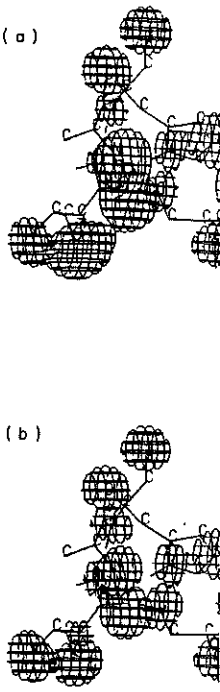

FIG. 2. 3-D Electrosta
on the backbone atoms
aspartic acid, $\varepsilon = 1$. (b),
$\varepsilon = |r - R_i|$.

aspartic acid and ε
and (iii) Asp 102 is
restrained the influe
of aspartic acid by
only to a small loc
sequently, for the ca
amino acids were kep

Previous studies o
ponctual net charge
approach; Nagy &
rested upon the c
approach; Gilson &
derived from the so
calculated at the CN
Mulliken population
yielded net charges

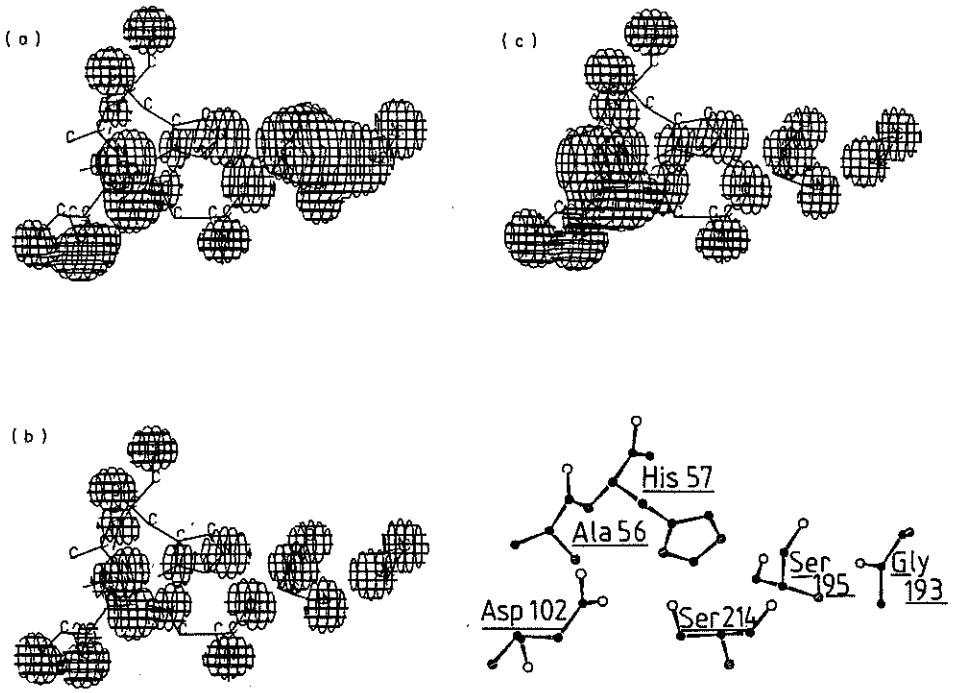

FIG. 2. 3-D Electrostatic potential isocontours at $-30\,\text{kcal mol}^{-1}$ generated by isolated net charges on the backbone atoms of the CHT1 model of the active site of chymotrypsin. (a), Residue 102 is an aspartic acid, $\varepsilon = 1$. (b), Residue 102 is an aspartic acid, $\varepsilon = |r - R_i|$. (c), Residue 102 is an aspartate, $\varepsilon = |r - R_i|$.

aspartic acid and $\varepsilon = |r - R_i|$ where R_i is the position vector of atom i [Fig. 2(b)]; and (iii) Asp 102 is aspartate and $\varepsilon = |r - R_i|$ [Fig. 2(c)]. As shown, ε considerably restrained the influence of every point charge [Fig. 2(a) and (b)] and replacement of aspartic acid by aspartate, with ε being a function of the distance $|r - R_i|$, led only to a small local difference around the carboxylate group of Asp 102. Consequently, for the calculation of $V(r)$ [eqn (2)] as it was made in this work, all the amino acids were kept neutral, thus simulating the presumed effect of the counterions.

COMPUTATIONAL METHODS

Previous studies on the electrostatic potential of macromolecules were based on ponctual net charges or made use of the bond contribution method (microscopic approach; Nagy & Naray-Szabo, 1985; Naray-Szabo & Nagy, 1985) and others rested upon the classical linearized Poisson-Boltzman model (macroscopic approach; Gilson & Honig, 1987). The electrostatic potentials presented below derived from the solution of eqn (2). The charge density matrix elements were calculated at the CNDO/2 level of approximation of Pople & Beveridge (1970). Mulliken population analysis of deorthogonalized molecular orbital coefficients yielded net charges that were close to the *ab initio* minimal basis set ones

(Pople *et al.*, 1965). The electrostatic potentials were computed within a complete CNDO scheme, and the nuclear attraction integrals were approximated by the opposite of the repulsion between *s* orbitals (approximation *I*, $\gamma_{\alpha H}$, hereafter called approximation γ, in Giessner-Prettre & Pullman, 1972). The map of the smallest CHT1 model of α-chymotrypsin (91 atoms) was also computed by explicit calculation of all mono-electronic integrals, using all the elements of the deorthogonalized CNDO density matrix (approximation IV in Giessner-Prettre & Pullman, 1972). A regular 3-D grid was calculated and the size of the box was that of the active site with a 3 Å increment in all directions. A contouring algorithm was used to join the points of identical energy level.

INFORMATIC TOOLS

The co-ordinates of the 25 water molecules selected from a Monte Carlo water bath were generated with the help of the Amber program (U. C. Singh, P. K. Weiner, J. Caldwell and P. A. Kollman, Department of Pharmaceutical Chemistry, University of California, San Francisco, CA, U.S.A.).

The monoelectronic electrostatic potential integrals were calculated using the links 301 and 604 of the program GAUSS70 (D. Peeters and M. Sana, Program DENPOT. University of Louvain, Louvain-la-Neuve, Belgium, Q.C.P.E., 360, Quantum Chemistry Program Exchange, Department of Chemistry, Indiana University, Bloomington, Indiana 47405, U.S.A.). The GAUSS70 algorithm which is 2·5 to three times faster than GAUSS82 as far as the link 604 is concerned, was adapted to an attached processor FPS 164, itself linked to a Digital VAX 11/780 computer. A program based on the calculation of the CNDO bielectronic integrals (and constructed by GD) allowed one to calculate a 3-D electrostatic potential map of $74 \times 75 \times 69$ points of the subtilisin active-site in 6555 *s* CPU time. This program was executed on the FPS 164. The contouring "Program PSI77" of W. L. Jorgensen (Purdue University, West Lafayette, Q.C.P.E. 340) was interfaced with the DI 3000 library and the electrostatic potential maps were displayed on a colour graphic processor Data General GDC 2400 with Conrac monitor.

Results and Discussion

In order to illustrate the 3-D electrostatic potential maps, isocontours at the -10 kcal mol^{-1} level defining wells of varying shape and volume are shown in Figs 3 and 4 for α-chymotrypsin and in Fig. 5 for subtilisin and the mutants Ser 125 → Ala and Ser 221 → Ala. Comparable views with the same orientation were produced by using the following orthogonal axes system. Axis *X* ran parallel to the direction

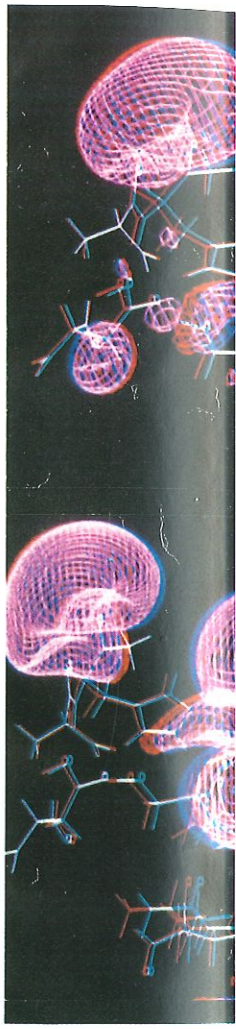

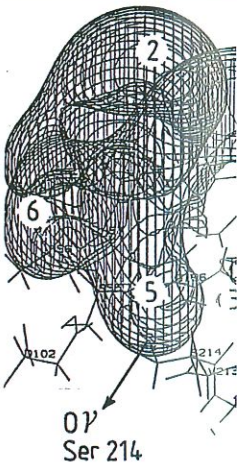

FIG. 3. 3-D Electrostatic potential isocontours at -10 kcal mol^{-1} generated by the active site of α-chymotrypsin using the atomic co-ordinates of Wipff *et al.* (1983) [(a)-(d) and (f)] and numbering of the wells (e). The electrostatic potential maps were calculated with approximation γ except that shown in Fig. 3(a), which was calculated with approximation IV. (a)–(b), Model CHT1; (c), model CHT2; (d) and (e), model CHT3; (f), model CHT3-25 H_2O. The water oxygen atoms are labelled. The stereoscopic effect is achieved using red (right eye) and green filters.

ed within a complete
approximated by the
$\gamma_{\alpha H}$, hereafter called
e map of the smallest
ed by explicit calcula-
the deorthogonalized
& Pullman, 1972). A
that of the active site
n was used to join the

a Monte Carlo water
C. Singh, P. K. Weiner,
Chemistry, University

calculated using the
nd M. Sana, Program
, Q.C.P.E., 360, Quan-
y, Indiana University,
m which is 2·5 to three
ed, was adapted to an
11/780 computer. A
tegrals (and construc-
ial map of $74 \times 75 \times 69$
rogram was executed
L. Jorgensen (Purdue
h the DI 3000 library
our graphic processor

s, isocontours at the
me are shown in Figs
mutants Ser 125 → Ala
on were produced by
rallel to the direction

ated by the active site of
and (f)] and numbering of
nation γ except that shown
HT1; (c), model CHT2; (d)
e labelled. The stereoscopic

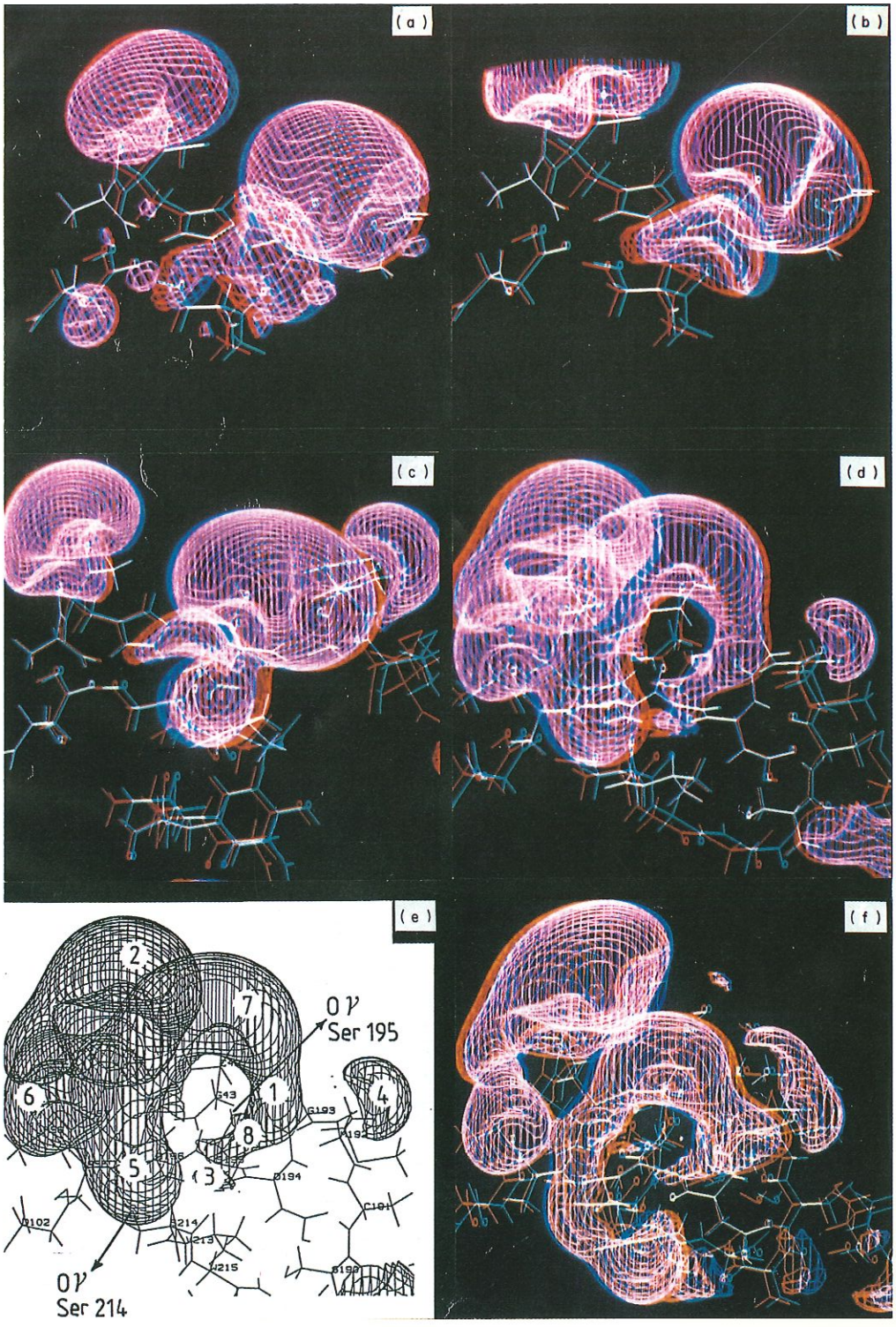

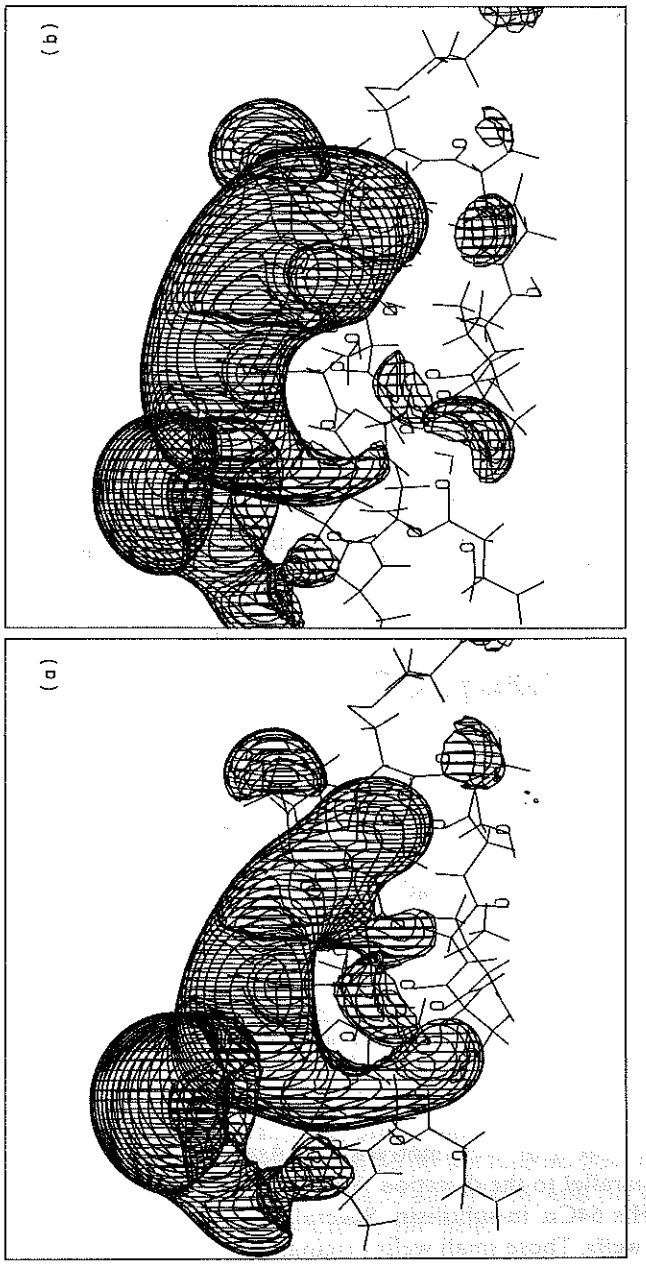

FIG. 4. 3-D electrostatic potential isocontours at -10 kcal mol^{-1} generated by the active site of α-chymotrypsin using the atomic co-ordinates of Tsukada & Blow (1985). (a), Model CHT3-TB; (b), model CHT3-TB-9 H_2O. The water oxygen atoms are labelled.

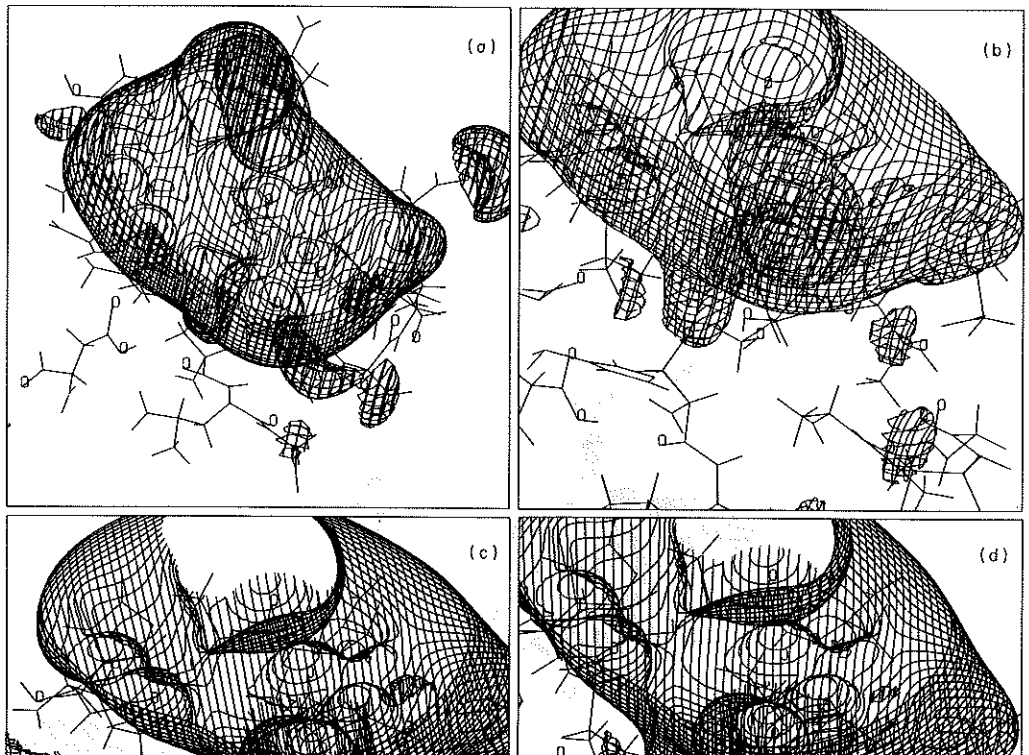

FIG. 5. 3-D Electrostatic potential isocontours at −10 kcal mole generated by the active site of subtilisin [(a) and (b)] and mutants Ser 125→Ala (c) and Ser 221→Ala (d). (a) Contains the 21 residues listed in Table 1. (b), (c) and (d) Focus on the active-site. In order to make the appendage of the pump more visible, the views were rotated by 10° along axis X. No changes were observed with mutant His 64→Ala (not shown).

Asp 102Cα → Ser 214Cα in α-chymotrypsin or Asp 32Cα → Ser 125Cα in subtilisin and axis Y ran parallel to the direction Asp 102Cα → His 57Cα in α-chymotrypsin or Asp 32Cα → His 64Cα in subtilisin. Several maps show isolated and marginally located negative wells. These small wells originated from the ends of the polypeptide chain segments that were selected to define the enzyme active sites.

The map of the CHT1 model of α-chymotrypsin was computed using approximation IV Giessner-Prettre & Pullman (1972) [Fig. 3(a)] and approximation γ [Fig.

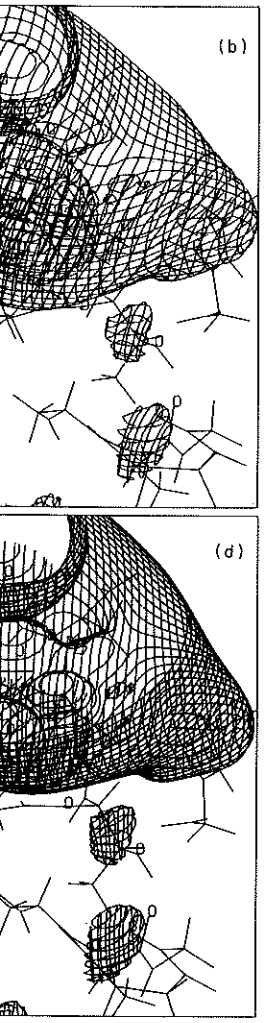

the active site of subtilisin
ins the 21 residues listed
ndage of the pump more
with mutant His 64→Ala

125Cα in subtilisin
in α-chymotrypsin
ated and marginally
ls of the polypeptide
sites.
uted using approxi-
proximation γ [Fig.

3(b)]. The shape, volume and disposition of the negative wells compared remarkably well, thus justifying the use of the much faster approximation γ procedure.

THE NUCLEOPHILIC SUCTION PUMP

The most salient feature of the 3-D electrostatic potential maps is the impressive negative volume or nucleophilic suction-pump that is generated by the enzyme active sites. The term suction-pump is suggested by the shape of the cloud. This volume bears a narrow funnel which is located in the immediate vicinity of the active site Ser 195 in α-chymotrypsin or Ser 221 in subtilisin and which orients itself towards Ser 214 in α-chymotrypsin or Ser 125 in subtilisin.

The co-operative effect of multiple amino acids

The stepwise construction of the map of the active-site of α-chymotrypsin, from model CHT1 to model CHT3, illustrates how the carbonyl groups of ten amino acids of the polypeptide backbone (Cys 42, Ala 55, Ala 56, His 57, Met 192, Gly 193, Asp 194, Ser 195, Gly 196, Ser 214) co-operatively shape up the nucleophilic suction-pump [Fig. 3(b)-(e)].

The minimal model CHT1 has three negative wells [Fig. 3(b)]. Well 1 (upper right) is generated by the carbonyl groups of the active-site Ser 195 itself and that of Gly 193, well 2 (upper left) by those of Ala 56 and His 57, and well 3 by that of Ser 214.

Model CHT2 has two additional wells [Fig. 3(c)]. Well 4 is generated by the carbonyl group of Met 192 and well 5 by that of Gly 196. Note that the triad Gly 226 Val 227 Tyr 228 which is located on the boundary of the cleft, does not contribute to the map at the selected -10 kcal mol^{-1} level.

Model CHT3 lacks this triad but has the completed stretches Cys 42-Cys 58 and Ser 190-Gly 196. It contains three additional wells [Fig. 3(d)]. Well 6 generated by the carbonyl group of Ala 55 fuses with wells 2 and 5. Well 7 generated by the carbonyl group of Cys 42 fuses with wells 1 and 2. Finally, well 8 generated by the carbonyl group of Asp 194 reshapes well 1 so that the bottom of the nucleophilic suction-pump is channelled towards the Oγ of the active-site Ser 195. Given the 7 Å sphere radius around Ser 195 used for the calculations, any expansion of the radius might affect the shape of the pump only at distances far away from the centre of the sphere.

Effects of atomic co-ordinates

When compared to model CHT3 [Fig. 3(d)], model CHT3-TB [Fig. 4(a)] shows only two slight modifications: (i) wells 5 and 6 do not fuse because of a modification in the backbone dihedral angle between Ala 55 and Ala 56; and (ii) well 1 is enlarged because of a rotation of the Asp 194 carboxylic head.

Effects of water

Completion of model CHT3 [Fig. 3(d)] with 25 water molecules, yielding model CHT3-25 H_2O of Fig. 3(f), causes extension of well 5. This extension is attributable

to three water molecules that are located close to the β-pleated sheet. In turn, completion of model CHT3-TB [Fig. 4(a)] with nine crystallization water molecules, yielding model CHT3-TB-9 H_2O of Fig. 4(b), modifies the shape of both wells 1 and 8 (in the vicinity of Ser 125) and prevents well 5 from extending towards the β-pleated sheet.

Effects of point mutations

Mutations also allow to dissect the relative contribution of individual residues to the 3-D electrostatic potential map. In subtilisin [Fig. 5(a) and (b)], channelling of the nucleophilic suction-pump towards the Oγ of Ser 125 is due to the contribution of the backbone carbonyl groups of Val 68 and the active-site Ser 221. As expected, Ala replacement of Ser 125 reduces the size of this appendage [Fig. 5(c)]. Mutations in the catalytic triad with single Ala replacement of Ser 221 and His 64 do not alter the shape of the pump at the -10 kcal mol^{-1} level, but the Ser 221 → Ala mutation allows the $N\varepsilon$ His 64 to create a small, additional, negative well outside the pump [Fig. 5(d)]. This observation is not surprising since the Oγ of Ser 221 in native subtilisin interacts with this imidazole $N\varepsilon$ group.

Slight modifications of the shape of the pump are likely to have minor effects on binding. In agreement with this view, the mutations Ser 221 → Ala and His 64 → Ala in subtilisin cause only minor effects on the Michaelis constant with the substrate N-succinyl-L-Ala-L-Ala-L-Pro-L-Phe-*p*-nitroanilide (Carter & Wells, 1988).

THE DIPOLE MOMENT

The nucleophilic suction-pump occupies mainly one side of the active-sites of α-chymotrypsin and subtilisin. This asymmetry is made especially conspicuous in Fig. 6(a) and (b) which were obtained by rotating the views of Fig. 3(d) of α-chymotrypsin and Fig. 5(a) of subtilisin, respectively. This asymmetry is directly related to the large value of the dipole moment which is the first term of the serial expansion of the electrostatic potential. In subtilisin, the main component of the dipole vector is oriented parallel to axis *Y*. In chymotrypsin, the dipole moment has two main components along axes *X* and *Y* (Table 2).

The polarization of the enzyme active-sites is a direct consequence of the asymmetrical distribution of the secondary structures. One part of the active-sites mainly consists of turns and other folded conformations that permit fusion of the individual negative clouds and generation of large negative wells. Conversely, the other part of the active-sites mainly contains β-strands. Their carbonyl groups protrude in an alternate manner on both sides of the backbone, thus preventing conjugation of the corresponding negative clouds through the molecular plane. Hence, the β-sheets that define part of the active sites of the serine peptidases not only serve as substrate binding sites, but also play an important role in building up a large dipole moment.

THE ELECTROPHILE

In α-chymotrypsin, as discussed above, the backbone carbonyl groups of Met 192 Gly 193 Asp 194 Ser 195 and Gly 196 contribute to the shape of the nucleophilic

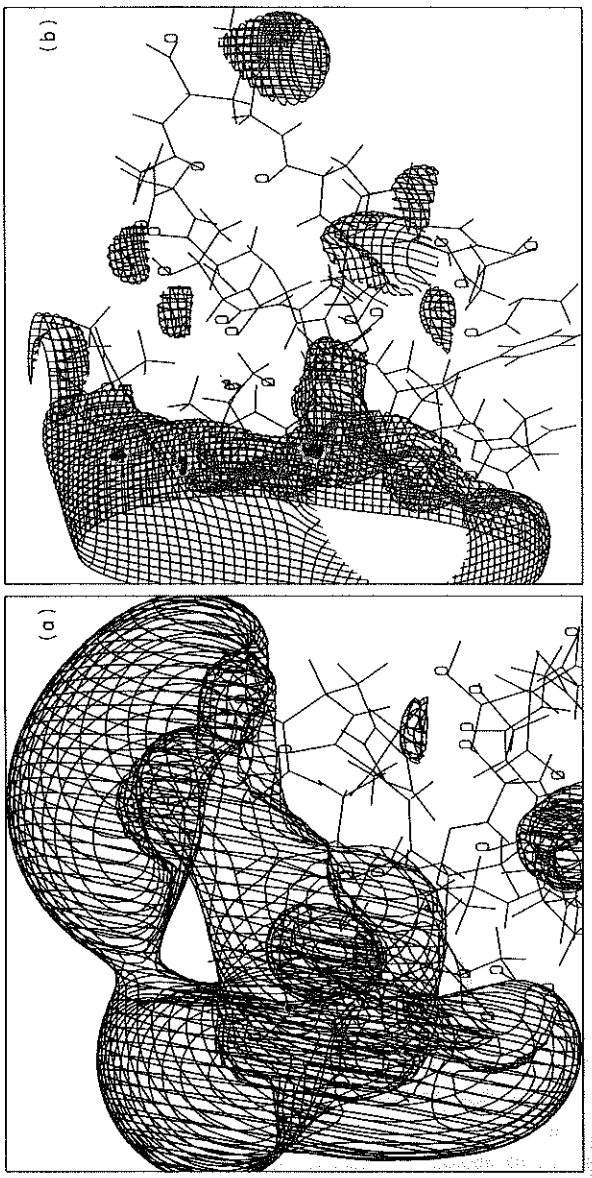

FIG. 6. 3-D Electrostatic potential isocontours at -10 kcal mol^{-1} generated by the active-site of α-chymotrypsin (a) and subtilisin (b). (a) and (b) were obtained by rotating by 90° around the Y axis the views of Figs 3(d) and 5(a), respectively.

TABLE 2

CNDO/2 dipole moment components (Debyes). The axes orientations are defined in the text

Enzyme	X	Y	Z	Total
Chymotrypsin	15·96	19·9	−7·76	26·69
Subtilisin				
Native	2·88	34·96	−0·21	35·07
Mutant Ser 125 Ala	3·26	33·23	−0·97	33·41
Mutant Ser 221 Ala	3·67	34·31	1·38	34·53
Mutant His 64 Ala	5·80	37·75	2·93	38·31

suction pump in the vicinity of the active-site Ser 195. In turn, the backbone NH groups of Gly 193 and Ser 195 of the same sequence serve as electrophilic hole or oxyanion binding site. In order to illustrate the location of this electrophilic hole, the 3-D electrostatic potential map of the tetrapeptide Ala Gly Gly Ser (at the end of which a $COCH_3$ group replaces the carboxylate) having the conformation of the tetrapeptide backbone Met 192 Gly 193 Asp 194 Ser 195 in α-chymotrypsin, was calculated using approximations IV and γ. Figure 7 is a 2-D map obtained with approximation γ. In addition to the isolated negative cloud generated by the carbonyl

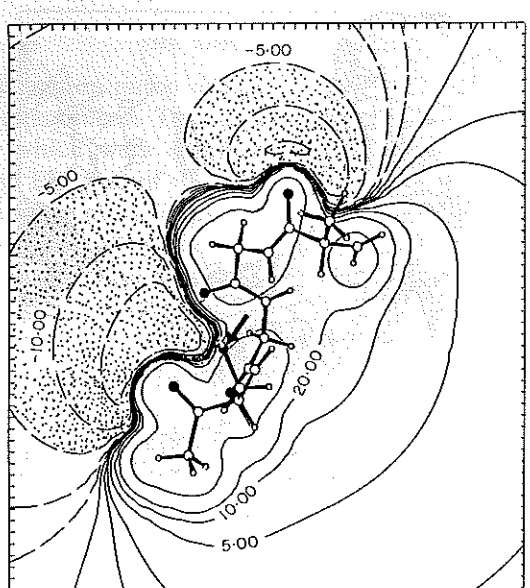

FIG. 7. 2-D Electrostatic potential isocontours, in kcal mol^{-1}, generated by the tetrapeptide Ala Gly Gly Ser in the conformation adopted by the tetrapeptide backbone Met 192 Gly 193 Asp 194 Ser 195 in α-chymotrypsin. The backbone NH groups of Gly 193 and Ser 195 are in the plane of the map. The carbonyl of Ser 195 is substituted by a methyl. The arrow indicates the Oγ of Ser 195.

group of Ala (Met) 192, the carbonyl groups of Gly 193, Gly (Asp) 194 and Ser 195 co-operatively create a much larger negative well, the bottom of which is oriented towards the Oγ of Ser 195. In turn, the backbone NH groups of Gly 193 and Ser 195 occur at the bottom of a positive well on the other side of the map, thus achieving a perfect complementation between the electrophilic hole and the nucleophilic suction-pump. Such a structural feature may be a common property of all the serine peptidases of the trypsin family.

In subtilisin, the active-site electrophilic environment is generated by the backbone NH of the active site Ser 221 and the side-chain amide group of Asn 155. In the native enzyme, this side-chain is not located close to the backbone NH of Ser 221. Hence, in contrast to α-chymotrypsin, the nucleophilic environment of the active-site serine in subtilisin has no effective electrophilic counterpart. However, upon binding with a suitable ligand, the Asn 155 side chain can undergo rotation (Poulos *et al.*, 1976; see also Carter & Wells, 1988: Fig. 3). Its amide group becomes oriented towards the oxyanion of the bound ligand while the negative well associated with its carbonyl group may fuse with and complete the nucleophilic suction-pump.

Conclusion

This paper describes the topology and electronic effects of the nucleophilic suction-pump and its electrophilic counterpart in the active sites of two serine peptidases belonging to distinct families. The picture depends of course on the crystallographic data used for the calculations. But, as illustrated, small variations in the atomic co-ordinates, the absence or the presence of water, the way the water molecules are distributed in the active sites and the occurrence of point mutations in the amino acid sequences have small effects on the shape of the electrostatic potentials.

The electrostatic potential map of the active-site of the serine peptidases can be regarded as a complexation index, with the nucleophilic suction-pump acting as a magnet towards the electrophilic part of the peptide ligand. Calculation of the electrostatic potential is an important step in the understanding of how these enzymes recognize their ligands, since the electrostatic interactions are the driving forces involved in the formation of non-covalent Michaelis complexes. However, as soon as bond formation and breaking occur, the electrostatic properties of the partners are not sufficient to describe the system. When the atomic distances between partners are above 2·5 Å, the electrostatic interaction energy is the most important component of the interaction energy and can be calculated by integrating the electronic density of one partner in the electrostatic potential of the other. The required numerical integration procedure has been developed (Dehareng *et al.*, 1989). At distances below 2·5 Å, and before any covalent linkage is broken or formed, correction terms must be introduced in the expression of the interaction energy.

This work was supported in part by the Fonds de la Recherche Scientifique Médicale (contract no. 3.4507.83), an Action concertée with the Belgian Government (convention 86/91-90), a convention with the Région wallonne (C2/C16/Conv.246/20428), the Fonds de Recherche de la Faculté de Médecine ULg and a contract with the EEC (BAP-0197-B).

REFERENCES

BIRKTOFT, J. J. & BLOW, D. M. (1972). *J. molec Biol.* **68,** 187–240.

CARTER, P. & WELLS, J. A. (1988). *Nature, Lond.* **332,** 564–568.

DEHARENG, D., DIVE, G., LAMOTTE-BRASSEUR, J. & GHUYSEN, J. M. (1989). *Theor. Chim. Acta, Berlin* **26,** 85–94.

DRENTH, J., HOL, W. G. J., JANSONIUS, J. N. & KOEKOEK, R. (1972). *Eur. J. Biochem.* **26,** 177–181.

GIESSNER-PRETTRE, C. & PULLMAN, A. (1972). *Theor. Chim. Acta, Berlin* **25,** 83–88.

GILSON, M. K. & HONIG, B. H. (1987). *Nature, Lond.* **330,** 84–86.

NAGY, P. & NARAY-SZABO, G. (1985) *J. molec. Struct. (Theochem)* **123,** 413–419.

NARAY-SZABO, G. & NAGY, P. (1985). In: *Molecular Basis of Cancer,* Part B: *Macromolecular Recognition, Chemotherapy and Immunology.* pp. 105–113. New York: Alan R. Liss.

POPLE, J. A. & BEVERIDGE, D. L. (1970). *Approximate Molecular Orbital Theory.* New York: McGraw Hill.

POPLE, J. A., SANTRY, D. P. & SEGAL, G. A. (1965). *J. chem. Phys.* **43,** S129–S135.

POULOS, T. L., ALDEN, R. A., FREER, S. J., BIRKTOFT, J. J. & KRAUT, J. (1976). *J. biol. Chem.* **251,** 1097–1103.

RAO, S. N., SINGH, U. C., BASH, P. A. & KOLLMAN, P. A. (1987). *Nature, Lond.* **328,** 551–554.

TSUKADA, H. & BLOW, D. M. (1985). *J. molec. Biol.* **184,** 703–711.

WARSHEL, A. & LEVITT, M. (1976). *J. molec. Biol.* **103,** 227–249.

WELLS, J. A. & ESTELL, D. A. (1988). *TIBS* **13,** 291–297.

WIPFF, G., DEARING, A., WEINER, P. K., BLANEY, J. M. & KOLLMAN, P. A. (1983). *J. Am. Chem. Soc.* **105,** 997–1005.